

# PubDAS: a PUBLIC Distributed Acoustic Sensing datasets repository for geosciences

Zack J. Spica<sup>1</sup>, Jonathan Ajo-Franklin<sup>2</sup>, Gregory C. Beroza<sup>3</sup>, Biondo Biondi<sup>3</sup>,  
Feng Cheng<sup>2</sup>, Beatriz Gaite<sup>4</sup>, Bin Luo<sup>3,α</sup>, Eileen Martin<sup>5</sup>, Junzhu Shen<sup>6</sup>,  
Clifford Thurber<sup>7</sup>, Loïc Viens<sup>1,β</sup>, Herbert Wang<sup>7</sup>, Andreas Wuestefeld<sup>8</sup>, Han  
Xiao<sup>9,γ</sup>, Tiejuan Zhu<sup>6</sup>.

<sup>1</sup>Department of Earth and Environmental Sciences, University of Michigan, Ann Arbor, MI, USA.

<sup>2</sup>Department of Earth, Environmental, and Planetary Science, Rice University, Houston, TX, USA.

<sup>3</sup>Department of Geophysics, Stanford University, Stanford, CA, USA.

<sup>4</sup>National Geographic Institute of Spain, Madrid, Spain.

<sup>5</sup>Colorado School of Mines, Golden, CO, USA

<sup>6</sup>Department of Geosciences, The Pennsylvania State University, State College, PA, USA.

<sup>7</sup>Department of Geoscience, University of Wisconsin–Madison, Madison, WI, USA.

<sup>8</sup>NORSAR, Kjeller, Norway.

<sup>9</sup>Department of Earth Science and Earth Research Institute, University of California, Santa Barbara,  
Santa Barbara, CA, USA.

<sup>α</sup>Now at Southern University of Science and Technology, Shenzhen, China

<sup>β</sup>Now at Los Alamos National Laboratory, Los Alamos, NM, USA.

<sup>γ</sup>Now at California Technological Institute, Pasadena, CA, USA

**Note:** This is a non-peer reviewed preprint submitted to EarthArXiv. It has also been  
submitted to Seismological Research Letters for peer review and publication  
consideration. If it is accepted, the EarthArXiv will be appropriately updated to reflect  
its publication status.

---

Corresponding author: Zack Spica, [zspica@umich.edu](mailto:zspica@umich.edu)

## 24 **Abstract**

25 During the past few years, Distributing Acoustic Sensing (DAS) has become an invaluable  
26 tool for recording high-fidelity seismic wavefields with great spatiotemporal resolu-  
27 tions. However, the considerable amount of data generated during DAS experiments  
28 limits their distribution with the broader scientific community. Such a bottleneck inher-  
29 ently slows down the pursuit of new scientific discoveries in geosciences. Here, we intro-  
30 duce PubDAS, the first large-scale open-source repository where several DAS datasets  
31 from multiple experiments are publicly shared. PubDAS currently hosts eight datasets  
32 covering a variety of geological settings (e.g., urban centers, underground mine, seafloor),  
33 spanning from several days to several years, offering both continuous and triggered ac-  
34 tive source recordings, and totalling up to  $\sim 90$  Tb of data. This manuscript describes  
35 these datasets, their metadata, and how to access and download them. Some of these  
36 datasets have only been shallowly explored, leaving the door open for new discoveries  
37 in Earth sciences and beyond.

## 38 **1 Introduction**

39 Seismology is an observational science heavily reliant on massive time series datasets.  
40 Seismologists typically use seismograms to image the Earth's interior and to understand  
41 its dynamic processes. Depending on the instrument, most seismic sensors measure ground  
42 motion in terms of acceleration, velocity, or displacement. Some instruments are equipped  
43 with one vertical and two orthogonal horizontal channels to characterize the vector com-  
44 ponents of ground motion. In all cases, seismometers record the ground motion at a par-  
45 ticular place as a function of time. The perception of how the Earth properties vary across  
46 measurement sites is often not characterized, except in rare experiments utilizing dense  
47 arrays.

48 Global and regional seismic networks provide high-quality waveforms over a broad range  
49 of frequencies. Some networks have been installed for several decades and have consid-  
50 erably advanced our knowledge of the Earth's interior (Lay et al., 1998; Ritsema et al.,  
51 1999; Boué et al., 2013). However, they suffer from poor scalability as their deployment,  
52 maintenance, and operation require great and ongoing effort and resources, particularly  
53 in remote areas. In the last decade we have seen a shift in seismic instrumentation with  
54 the development of cheap, portable, and stand-alone geophones (Hammond et al., 2019).  
55 Although they provide lower quality measurements, seismologists have used them to ob-

56     tain dense spatial coverage, useful for unravelling the complexity of fault zones, sedimen-  
57     tary basins, or volcanoes (Schmandt & Clayton, 2013; Mordret et al., 2013; Ben-Zion et  
58     al., 2015; Z. Spica et al., 2018; Castellanos et al., 2020). Overall, we are seeing an ac-  
59     celeration in the rate of data acquisition and increasingly higher density measurements,  
60     facilitated by advances in autonomous sensors (e.g., "nodal seismometers") and other  
61     new techniques (e.g., Ben-Zion et al., 2015; Sweet et al., 2018). As a result, the seismic  
62     data available for download on the Incorporated Research Institutions for Seismology  
63     (IRIS) Data Management Center (DMC) is growing at an exponential rate (e.g., Kong  
64     et al., 2019). As of April 1<sup>st</sup>, 2022, the IRIS-DMC hosted  $\sim 882$  TB (IRIS, 2022), and  
65     following the current trend, we expect it to double in the next three years. Yet, this trend  
66     is expected to accelerate further due to the rapid emergence of a new seismic measure-  
67     ment method called Distributed Acoustic Sensing (DAS; Fig. 1).

68     DAS is a measurement technology that turns fiber-optic cables into ultra-dense arrays  
69     of sensors measuring real-time vibrations at high sampling rate (Hartog, 2017). It mea-  
70     sures high-fidelity wavefields over tens of kilometers – a product that was previously only  
71     possible through industrial seismic experiments. For a given time period, DAS datasets  
72     can produce orders of magnitude more data than traditional passive seismic experiments.  
73     For example, the Fiber-Optic Sacramento Seismic Array (FOSSA) experiment (J. B. Ajo-  
74     Franklin et al., 2019) recorded seven months of continuous wavefield at 500 Hz, every  
75     2 m and over 25 km, and generated close to  $\sim 300$  Tb of raw and minimally processed  
76     secondary data (Fig. 1C). This dataset alone would represent  $\sim 34\%$  of the total current  
77     IRIS-DMC database if it were hosted there. The rapid data accumulation resulting from  
78     recent DAS experiments is poised to intensify in the coming years given the wider avail-  
79     ability and decreasing cost of DAS interrogators (Lindsey & Martin, 2021). The antic-  
80     ipated petabyte-per-year influx and the lack of policies in place regarding information  
81     technology and national security requirements (e.g., Federal Communications Commis-  
82     sion, United States Navy) put public data centers in a challenging position as they can-  
83     not currently accept large DAS data inflows.

84     Public data centers are the cornerstone of open science. They strive to share data, knowl-  
85     edge, and information within the scientific community and the wider public thereby stim-  
86     ulating scientific research and advancing our understanding of the world (Ramachandran  
87     et al., 2021). Accordingly, many institutions and even scientific journals have adopted  
88     policies that encourage or require scientists to make data available through such data

89 centers. Public data within seismology and applied geophysics is typically disseminated  
90 by way of the IRIS-DMC for US National Science Foundation (NSF) sponsored research  
91 or by special repositories maintained by other federal sponsors including US Department  
92 of Energy’s with the Energy Data Exchange (EDX; U.S. Department of Energy, 2022a)  
93 and Geothermal Data Repository (GDR; U.S. Department of Energy, 2022b). For re-  
94 search funded outside of these organizations, no cost-effective options are available for  
95 making datasets in the 10s to 100s of TB scale publicly accessible, given the existing fi-  
96 nancial and structural models of general purpose repositories. The current bottleneck  
97 on public seismic data archives slows pursuit of exciting scientific discoveries that might  
98 be facilitated by existing, but inaccessible, DAS datasets. This is further exacerbated  
99 by the fact that access to DAS instrumentation is exclusive to a few research groups that  
100 can either afford to purchase or rent an instrument. Currently, community instrument  
101 pools are considering avenues to support DAS instrument access. Public data archive  
102 infrastructure has yet to be created to match these instrumentation investments.

103 In this paper we introduce PubDAS, a public repository presently hosting 8 DAS datasets,  
104 for a total of  $\sim 90$  Tb. In the near-future, we expect PubDAS to grow and ultimately mi-  
105 grate toward well-established data centers. However, as it stands today, PubDAS aims  
106 to temporarily help the seismological community find a home for critical DAS datasets  
107 and hopefully foment discoveries in Earth sciences. The datasets cover a variety of ge-  
108 ological settings (e.g., urban centers, underground mine, seafloor) and some datasets are  
109 continuous, spanning from several days to several years (Fig. 1A) while others provide  
110 triggered active source recordings. We expect that these datasets will have applications  
111 beyond the purposes for which they were originally recorded.

112 In the following sections, we first review the working principles of DAS and its current  
113 fields of application in Earth sciences. We then present the main characteristics of the  
114 different datasets and discuss their metadata. Then, we describe how to access PubDAS  
115 and discuss other DAS datasets already available online. To conclude, we discuss future  
116 steps and envision the broader impact that PubDAS could have for the geoscience com-  
117 munity.

## 118 **2 Overview of the DAS Recording Systems**

119 DAS systems are a combination of an interrogator unit (IU) connected to a standard fiber  
120 cable (i.e., single-mode) and a data storage unit. While the interrogator unit in its sim-

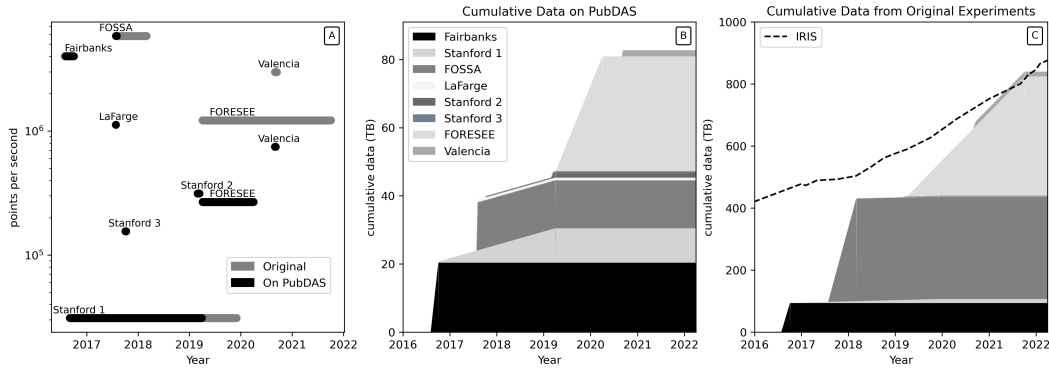


**Figure 1.** A) Time span versus data points per second for all experiments available in PubDAS. Some datasets are provided in full, some have been trimmed, and others have been down-sampled to keep a reasonable data volume shown in (B). B) Cumulative data volume for all the datasets available on PubDAS. D) Cumulative data volume for all original datasets and comparison with the data volume available for download from the IRIS-DMC (IRIS, 2022). Fairbanks: Fairbanks Permafrost Experiment array; FORESEE: Fiber-Optic foR Environment SEnsEing array; FOSSA: Fiber Optic Seismic Super Array; LaFarge: LaFarge-Conco Mine array; Stanford 1: Stanford campus array; Stanford 2: Sandhill Road Array; Stanford 3: Stanford Campus with two IUs; Valencia: Valencia Array.

121 plest form is an optical interferometer, the cable serves as both a distributed extensional  
 122 strain (or strain rate) sensor and a means of transmitting its own data to the storage unit.  
 123 The interrogator unit probes the cable via short pulses of laser light and typically mea-  
 124 sures the Rayleigh back-scattered photons over successive fiber segments. The zone of  
 125 the fiber that the pulse averages over is referred to as a gauge length. When the fiber  
 126 is stationary, such Rayleigh backscattering is constant; however, when the fiber is dis-  
 127 torted due to a vibration, the resulting phase shift is quasi-linearly proportional to the  
 128 changes in path length over the gauges (Grattan & Sun, 2000). The gauge length de-  
 129 fines the spatial resolution of the measurement, while the channel spacing defines the mea-  
 130 surement density. Typically, both the gauge length and the channel spacing can vary from  
 131  $\sim 5$  to  $\sim 40$  m and from  $\sim 0.25$  to  $\sim 20$  m, respectively. Note that channels may overlap  
 132 if the gauge length is larger than the channel spacing. Depending on the manufactur-  
 133 ing design, the IU may operate in the time or the frequency domain and record vibra-  
 134 tion information either in terms of strain or strain-rate, accordingly.

135 Even though the technology is constantly improving, in some cases approaching the qual-  
136 ity of classical inertial sensors (e.g., geophones) on a point-for-point basis, there are trade-  
137 offs and drawbacks that can interfere with data when selecting recording parameters. For  
138 example, a larger gauge length lowers spatial resolution but may also decrease statisti-  
139 cal uncertainty in measurements over the gauges (E. R. Martin, 2018). In addition, the  
140 gauge length has an effect on the amplitude response by generating zero strain notches  
141 at frequencies that are a multiple of the gauge length (Dean et al., 2017; Jousset et al.,  
142 2018; Lindsey, Rademacher, & Ajo-Franklin, 2020). Except in special cases, DAS typ-  
143 ically has a lower signal-to-noise ratio (SNR) and a more limited angular sensitivity than  
144 standard geophones (E. R. Martin, Lindsey, et al., 2018). In addition, both the fibers  
145 and the cables (one or several fibers are enclosed in a cable) vary in design depending  
146 on several technical and logistical requirements (Soga & Luo, 2018). While the optical  
147 fiber composed of coated silica glass controls the light propagation, the cable has an im-  
148 pact on the coupling with the ground (Daley et al., 2013) and can impact data quality.  
149 These drawbacks are largely compensated by the benefits of having ultra-dense time se-  
150 ries of permanently installed and highly resistant seismic sensors in logistically challeng-  
151 ing locations, communicating over large distances and running on a single power source  
152 (E. R. Martin, Lindsey, et al., 2018).

153 There are many more technical details about DAS measurements and their comparison  
154 to standard instruments (e.g., Papp et al., 2017; Wang et al., 2018; Z. J. Spica, Pertou,  
155 et al., 2020; van den Ende & Ampuero, 2021). In this communication, we only describe  
156 the basic working principle to note that depending on the IU and the input parameters,  
157 the recorded data are specific to each experiment. All these parameters and cable char-  
158 acteristics (when known) should be taken into account in data processing and interpre-  
159 tation. For an extensive overview of the working principles of DAS, we refer the reader  
160 to (Hartog, 2017).

### 161 **3 Overview of the current fields of application in Earth sciences**

162 The vast majority of seismic recordings with DAS were initially operated by the energy  
163 industry with many pilot experiments performed in downhole environments (e.g., Mes-  
164 tayer et al., 2011; Parker et al., 2014; Lellouch, Horne, et al., 2019; Y. Li et al., 2021).  
165 Rapidly, particular attention was paid to repeatable vertical seismic profile imaging (Molenaar  
166 et al., 2012; Daley et al., 2013; Mateeva et al., 2012; Mateeva, Lopez, et al., 2013; Ma-

167 teeva, Mestayer, et al., 2013), micro-seismicity monitoring during hydraulic fracturing  
168 (Bakku, 2015; Karrenbach et al., 2017), and fluid flow monitoring through hydrocarbon  
169 production (Daley et al., 2013). It is only over the past few years that experiments started  
170 to focus on fibers deployed in the near surface with applications designed for shallow seis-  
171 mic characterization and passive seismology (Zhan, 2020). Since then, several applica-  
172 tions have demonstrated the consistency between earthquake waveforms recorded by DAS  
173 and conventional seismometers (e.g., Lindsey et al., 2017; Wang et al., 2018; J. B. Ajo-  
174 Franklin et al., 2019; Lindsey & Martin, 2021). Furthermore, the DAS instrument re-  
175 sponse appears to be broadband (e.g., Lindsey et al., 2017; Jousset et al., 2018; J. B. Ajo-  
176 Franklin et al., 2019; Lindsey, Rademacher, & Ajo-Franklin, 2020), which opens the door  
177 to imaging the Earth across different scales. For example, Yu et al. (2019) recorded earth-  
178 quake’s surface waves down to 200 s.

179 Among the many different fields of application, DAS has now been used to character-  
180 ize geothermal sites (Reinsch et al., 2015; Zeng et al., 2017; Lindsey et al., 2017; Lan-  
181 celle et al., 2021), the inside of the San Andreas fault (Lellouch, Yuan, et al., 2019b, 2019a),  
182 glaciers (Walter et al., 2020; Hudson et al., 2021; Fichtner et al., 2022), and densely pop-  
183 ulated urban centers (Lindsey, Yuan, et al., 2020; Z. J. Spica, Perton, et al., 2020; Yuan  
184 et al., 2020; Shragge et al., 2021; Zhu et al., 2021). It has also shown promise in the con-  
185 text of various monitoring applications, notably for detecting earthquakes (Lindsey et  
186 al., 2017; Z. Li & Zhan, 2018; Lellouch, Yuan, et al., 2019a), monitoring landslides (Iten,  
187 2012), recording volcanic activity (Klaasen et al., 2021; Currenti et al., 2021; Nishimura  
188 et al., 2021; Jousset et al., 2022), characterizing permafrost thaw (J. Ajo-Franklin et al.,  
189 2017; Cheng et al., n.d.), estimating blasts or explosions (Zhu et al., 2021; Mellors et al.,  
190 2021), and recording weather-ground events (Zhu & Stensrud, 2019; Shen & Zhu, 2021a).  
191 DAS recordings were also used for ambient noise interferometry (e.g., Zeng et al., 2017;  
192 E. R. Martin & Biondi, 2017), offering the possibility to retrieve repeatable signals (i.e.,  
193 Rayleigh and Love waves) for near-surface characterization (E. Martin, Biondi, Karren-  
194 bach, & Cole, 2017; J. B. Ajo-Franklin et al., 2019; Dou et al., 2017) and aquifer mon-  
195 itoring (Rodríguez Tribaldos & Ajo-Franklin, 2021). In addition, subsea telecommuni-  
196 cation fibers have been used to monitor ocean dynamics (Lindsey et al., 2019; Sladen et  
197 al., 2019; Williams et al., 2019, 2022) but also to detect earthquakes (Lior et al., 2021;  
198 Z. J. Spica et al., 2022) and acoustic phases (Rivet et al., 2021; Ugalde et al., 2022; Z. J. Spica  
199 et al., 2022), image the near-shore subsurface (Z. J. Spica, Nishida, et al., 2020; Z. J. Spica

200 et al., 2022; Cheng et al., 2021; Williams et al., 2021; Viens et al., 2022), assess detailed  
 201 nonlinear ground motion amplification (Viens & Spica, 2022), or precisely locate the sources  
 202 of microseisms (Xiao et al., 2022).

203 The former non-exhaustive list of studies suggest that DAS will likely play an important  
 204 role in seismology and many other fields in Earth sciences in the near future.

Name	IU	T. span (d)	Format	Sps (hz)	Vol. (Gb)	GL (m)	CL (m)	CS (m)	units
Fairbanks	iDAS	59*	TDSM	1,000	10,441	10	4,000	1	$\dot{\epsilon}$
FORESEE	iDAS-v2	365	HDF5	125 <sup>‡</sup>	29,338	10	4,900	2	$\dot{\epsilon}$
FOSSA	iDAS-v2	7	TDSM	500	11,680	10	23,300	2	$\dot{\epsilon}$
LaFarge	iDAS	2*	SEG-Y	1,000	45	10	1,120	1	$\dot{\epsilon}$
Stanford-1	ODH3	940	SEG-Y	50	18,908	7.14	2,500	8.16	$\epsilon$
Stanford-2	ODH3	14	SEG-Y	250	2,887	20	10,200	8.16	$\epsilon$
Stanford-3	ODH4	6	SEG-Y	~	92	~	2,500	8.16	$\epsilon$
Valencia	A1-R	7	HDF5	250 <sup>‡</sup>	3,213	30.4	50,000	16.8	$\dot{\epsilon}$

**Table 1.** List of the data sets currently available on PubDAS and their main characteristics. IU: Interrogator Unit; T. Span: Time span in days; Sps: Samples Per Second in Hertz; Vol.: Volume in Gigabytes; GL: Gauge Length in meters; CL: Cable Length in meters; CS: Channel Spacing in meters;  $\dot{\epsilon}$ : strain rate;  $\epsilon$ : strain; A \* means data contain active sources. A ~ means that this value may vary; <sup>‡</sup>: means the dataset is downsampled. Name abbreviations are the same as in Fig. 1.

#### 205 4 Characteristics of the repository

206 PubDAS currently includes 8 datasets recorded with different instruments and acqui-  
 207 sition settings (Fig. 1 and Table 1). All datasets provide continuous measurements from  
 208 several hours to several weeks. Possible gaps in the datasets originate from temporal record-  
 209 ing issues or were planned as such during field measurement. Most of the datasets are  
 210 provided in their raw original format as direct outputs from their respective IUs. The  
 211 two exceptions are the FORESEE and Valencia arrays, which have been downsampled  
 212 to 125 and 250 Hz, respectively, using a anti-aliasing low-pass filter. This is the only pre-  
 213 processing applied to these datasets. Table refT1 summarizes some of the key features  
 214 of the datasets.

#### 215 4.1 Fairbanks Permafrost Experiment Array

216 The Fairbanks Permafrost Experiment Array is located outside of Fairbanks, Alaska, on  
 217 the Fairbanks Permafrost Experiment Station/Farmer’s Loop Site, operated by the US  
 218 Army Corps of Engineer’s (USACE) Cold Regions Research and Engineering Labora-  
 219 tory (CRREL; Fig. 2). The array consists of a 2D grid of hybrid tactical fiber cables in-  
 220 stalled in trenches between 20 and 40 cm deep. The array was installed to monitor an  
 221 active heating experiment where a section of permafrost was thawed using an in-ground  
 222 heating system. DAS data were recorded on the array using both active and passive sources  
 223 for a period of 2 months during the thaw process.

224 The site and heating experiment are de-  
 225 scribed in (Wagner et al., 2018) while  
 226 the active source monitoring activities  
 227 are documented in (J. Ajo-Franklin et  
 228 al., 2017) and (Cheng et al., n.d.). The  
 229 data available on PubDAS are for the  
 230 four road parallel lines (A,B,C,D), each  
 231 approximately 180 m in length and travers-  
 232 ing the heating experiment, as well as  
 233 the five shorter road perpendicular lines  
 234 (1, 2, 3, 4, 5). The data were recorded  
 235 using an iDAS-v2 interrogator (Silixa LLC)  
 236 at 1 kHz and a 1 m spatial sampling with  
 237 a 10-m gauge length. Data is saved in  
 238 native measurement units (proportional  
 239 to strain rate). While both active and  
 240 passive data were acquired, the curated  
 241 PubDAS dataset is for the active exper-  
 242 iment which records sequential shots from a single Surface Orbital Vibrator (SOV), swept  
 243 multiple times every evening to allow for timelapse monitoring of environmental processes.  
 244 Geophone data recording the SOV sweeps, useful for deconvolution, are also archived.

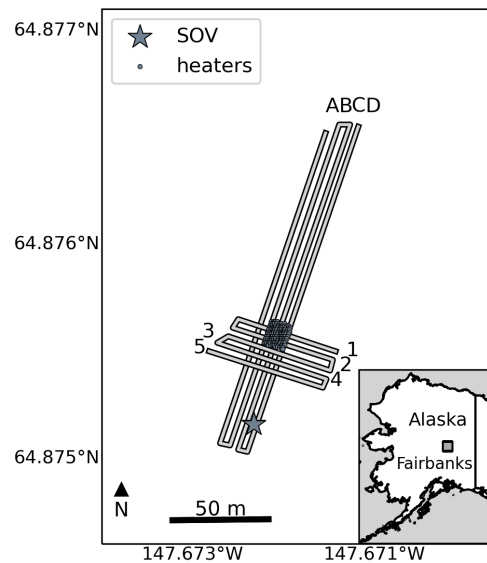


**Figure 2.** Map of the Fairbanks Permafrost Experiment Array. The letters and numbers refer to the line labels. Only the channels at the end of each line have been tap tested. SOV: Surface Orbital Vibrator.

## 4.2 The Fiber-Optic foR Environment SEnsEing (FORESEE) Array

The FORESEE array is located in central Pennsylvania in the Valley and Ridge Appalachians region (Fig. 3). The array consists of an iDAS-v2 interrogator and a  $\sim 5$ -km long single-mode dark fiber installed underneath the Pennsylvania State University campus. The fiber shown in Fig. 3 is made of two individual fibers that were spliced together around channel 1340. The cable sits in buried concrete conduit at depths ranging between 1 and 10 m. Continuous strain-rate measurements were performed between April 5, 2019, and October 4, 2022, with a 500 Hz sampling frequency, a 10-m gauge length, and 2-m channel spacing. The first 2137 channels along the cable have been accurately located with tap tests. The first third of the array (i.e., channels 1 to 604) is located in a quiet off-campus area and the rest of the array is on the main campus with stronger anthropogenic noise. Zhu et al. (2021) describe how to calibrate the DAS recordings to particle velocity using earthquake waveforms from a nearby broadband seismometer.

Throughout the 2.5-year experiment, the array recorded a variety of transient signals, including global and regional earthquakes, thunderquakes (Zhu & Stensrud, 2019; Hone & Zhu, 2021), and mining blasts (Zhu et al., 2021). In addition, anthropogenic signals common to urban environments were also detected, such as cars, footsteps, and live music events (Shen & Zhu, 2021b). The long duration of the experiment also allows exploration of the effect of seasonal environmental variations, and provides critical information on surface and subsurface processes.

In PubDAS, data acquired during the first year of the experiment (i.e., April 5, 2019 - March 14, 2020) are available. During this time, the recordings were interrupted several times due to unexpected power outages and data files were rewritten to keep consistency in hdf5 format during preprocessing. The FORESEE array is the largest dataset on PubDAS, even though the data have been downsampled from 500 Hz to 125 Hz.

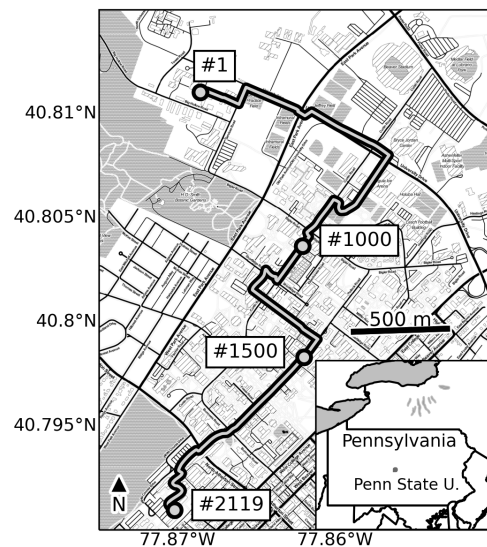


**Figure 3.** Map of the Fiber-Optic foR Environment SEnsEing (FORESEE) Array.

### 4.3 The Fiber Optic Seismic Super Array (FOSSA)

The FOSSA experiment was conducted on the Sacramento River flood plain, north and west of Sacramento, CA. The experiment utilized a 27 km section of dark telecommunications fiber, part of DOE's ESnet network, connecting West Sacramento with the town of Woodland (Fig. 4). Data of usable quality was recorded on approximately 23.3 km (11,648 sampling locations, 2m spacing). The experimental targets were monitoring regional seismicity and characterizing near-surface structure using ambient noise methods. Data were collected between July 28, 2017 and January 18, 2018, at an original sampling rate of 500 Hz, generating a total of 210 TB of raw uncompressed data. J. B. Ajo-Franklin et al. (2019) describe how some sections of the fiber were mapped using sequential impact tests at the surface and provide other details about the field installation of the equipment. As discussed in Rodríguez Tribaldos and Ajo-Franklin (2021), the cable was largely deployed within conduit buried in soil at depths of 1-1.5 m. Some sections were also placed in shallow horizontal boreholes beneath roads and railway tracks, again in conduit but slightly deeper (3 to 4 m). The response of the fiber was also explored through comparison to a co-located broadband inertial sensor by (Lindsey, Rademacher, & Ajo-Franklin, 2020) for both teleseismic events and microseism energy.

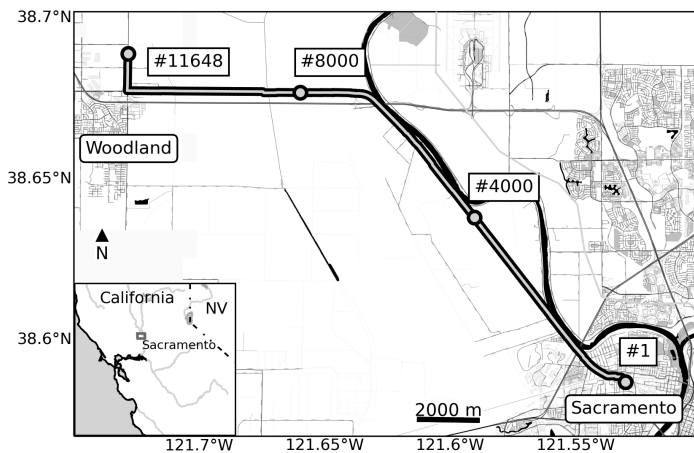


**Figure 4.** Map of the Fiber Optic Seismic Super Array (FOSSA).

After bending westward towards Woodland, the fiber follows Interstate 5. In addition, the cable is sometimes co-linear with a heavily used rail corridor. The surficial aquifer is influenced by both natural precipitation, irrigation, and river stage, which can influence soil properties; Rodríguez Tribaldos and Ajo-Franklin (2021) used the dataset to monitor the aquifers

The fiber used in the FOSSA experiment traverses several distinct settings of development with different installation and noise characteristics. The fiber starts in an urban area and continues into a section of farmland near the Sacramento River.

After bending west-

311 using ambient noise interferometry. The quality and diversity of the wavefield recorded  
 312 allowed Nayak et al. (2021) to produce mixed-sensor cross-correlation between regional  
 313 seismometers and strain-rate DAS recordings. In PubDAS at present, one week of con-  
 314 tinuous raw data that contains a variety of signals, including large teleseismic earthquakes,  
 315 is available for download.

#### 316 4.4 LaFarge-Conco Mine Array

317 The LaFarge-Conco mine is a Limestone and dolomite mine located in North Aurora,  
 318 IL (Fig. 5). The layout consists of north and south sections, which are connected by un-  
 319 derground passageways beneath Interstate 88. This room-and-pillar mine occupies a wedge-  
 320 shaped footprint that is approximately 1500-m long by 500-m wide at the I-88 dividing  
 321 line. The mine includes four levels down to a depth of about 80 m. Pillars are approx-  
 322 imately 20 meters on a side and in height. The rock is blasted from the formation most  
 323 weekdays in mid-afternoon. Rocks are then hauled by truck up a decline to the north-  
 324 west entrance for processing. Background noise from mine truck traffic and conveyor belts  
 325 is observed during the DAS experiment except when the mine was cleared for blasting.

326 The DAS array was located in the north  
 327 section of the first level of the mine as  
 328 shown in Zeng et al. (2021). A  $\sim 1120$   
 329 m of tactical fiber-optic cable was laid  
 330 down over three layers along an L-shape  
 331 loop. In loop 1, the cable was secured  
 332 in a groove cut in the floor using a pave-  
 333 ment saw and then covered with self-leveling  
 334 concrete. Two additional loops were placed  
 335 above the cemented cable. Loop 2 was  
 336 placed in the grove and covered with fine  
 337 rock powder, and in Loop 3 the top strand  
 338 was placed without cover. The DAS in-  
 339 terrogator was set up in a tent near a pil-  
 340 lar a few meters west of the cable lay-  
 341 out. Power was supplied by a generator  
 342 but batteries were used during blasting

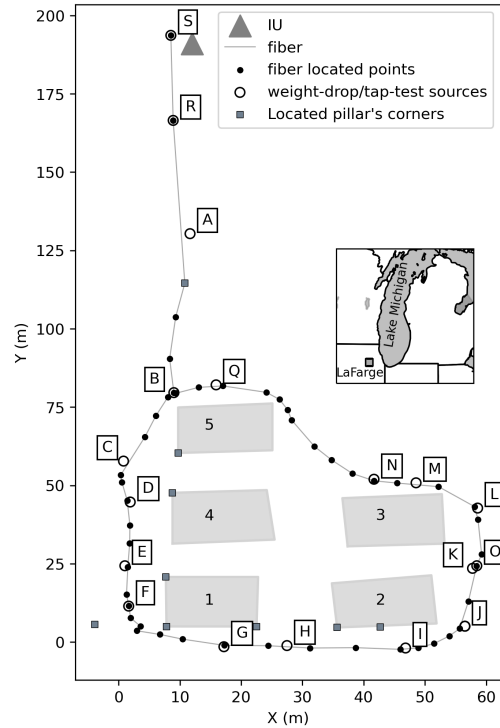


**Figure 5.** Map of the LaFarge-Conco Mine array. The numbered grey areas represent the mine pillars.

343 testing to limit vibrational noise. Sev-  
 344 eral locations along the DAS cable were  
 345 tap tested to associate the DAS channel number with the surface position of the cable  
 346 (Zeng et al., 2021). A 23-kg weight providing 208 J of energy was the seismic source at  
 347 the lettered stations in Fig. 5. Also, two mine blasts at distances of about 200 and 450-  
 348 m from the DAS array were used to test the feasibility of monitoring stress changes from  
 349 travel-time changes. The sharpest P-wave arrivals were recorded by the cemented ca-  
 350 ble and poorest arrivals were recorded by the loose cable.

#### 351 4.5 Stanford 1 – Stanford Campus Array:

352 The Stanford campus array in California (Fig. 6) was created using a fiber cable loosely  
 353 deployed in an air-filled PVC conduit ( $\sim 12$  cm wide) in the same way other fiber cables  
 354 are installed around campus. The fibers were pulled along these conduits accessible through  
 355 manholes (small underground rooms). The coupling between the cable and the surround-  
 356 ing medium relies exclusively on gravity and friction when the fiber sits in the conduits.  
 357 In manholes, the fiber was zip-tied to a bracket on the side of the wall. In addition, 45  
 358 m of fiber was spooled up and strapped to the wall (with a vertical and horizontal com-  
 359 ponent) at Campus Dr. and Via Ortega, and south of Allen on Via Pueblo. The fiber  
 360 location was calibrated with tap tests as described in details in (E. Martin, Biondi, Cole,  
 361 & Karrenbach, 2017). Continuous recordings were acquired using an OptaSense ODH-  
 362 3 IU at 50 Hz between September 2nd 2016 and March 31st 2019, for a total of 626 chan-  
 363 nels. With 940 days available for download, this dataset offers the longest time span in  
 364 PubDAS.

365 Through this exper-  
 366 iment, E. R. Martin  
 367 et al. (2017) and Biondi  
 368 et al. (2017) showed  
 369 that the DAS technol-  
 370 ogy can be used to record  
 371 seismic data directly  
 372 from a free-standing  
 373 telecommunication ca-  
 374 ble. The data from this

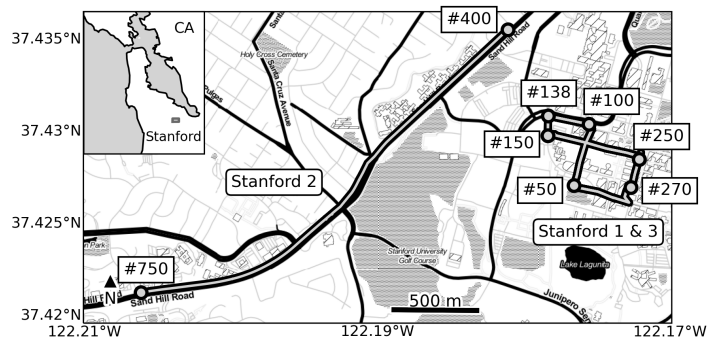


**Figure 6.** Map of the different Stanford arrays. Stanford 1 and 3 recorded the same fiber loop on main campus but with different IUs. Stanford 2 was recorded around Palo Alto.

375 array provide a unique  
376 opportunity to monitor long-term variations of the ambient seismic field generated by  
377 natural and anthropological sources (E. R. Martin & Biondi, 2018; E. R. Martin, Huot,  
378 et al., 2018; Huot et al., 2017), to analyze hundreds of earthquakes as well as numerous  
379 quarry blast waveforms (Biondi et al., 2017; Lindsey et al., 2017; Fang et al., 2020), to  
380 monitor infrastructure (Fang et al., 2020), and to image the shallow subsurface in a pop-  
381 ulated urban area (Z. J. Spica, Perton, et al., 2020). This dataset also enables extensive  
382 exploration of the application of machine learning and deep learning algorithms on high-  
383 volume DAS data for effective event detection and automatic data processing (e.g., Huot  
384 & Biondi, 2018).

#### 385 **4.6 Stanford 2 – Sandhill Road Array:**

386 Stanford 2, starting from December 2019, was the natural extension of Stanford 1. It scaled  
387 up the initial proof-of-concept of Stanford 1 array to a citywide deployment around Palo  
388 Alto, CA (Biondi et al., 2021). With a cable length of 10.2 km and a channel spacing  
389 of 8.16 m, the array counts a total of 1250 channels (Fig. 6). The data volume write rate  
390 was approximately 101 Gb/day. Two full weeks of raw data with all 1250 channels orig-  
391 inally sampled at 250 Hz and recorded between March 1 and 14, 2020 are available on  
392 PubDAS. About 350 channels were located along the relatively straight Sandhill Road  
393 section between the quiet portion of the array near Stanford Hospital (Channel #400)  
394 and SLAC (Channel #750). The section of the array between channels 400 and 750 (Fig.  
395 6) provides the highest SNR. The location of the channels along this segment were cal-  
396 ibrated by driving a dedicated car at constant velocity at night along the fiber (Yuan  
397 et al., 2020). Lindsey, Yuan, et al. (2020) used this array to detect hundreds of thousands  
398 of individual vehicles and monitor urban activity levels during the early stages of the COVID-  
399 19 pandemic. (Yuan et al., 2020) investigated a cost-effective urban infrastructure mon-  
400 itoring system by combining Vehicle Onboard Sensing (VOS) and roadside DAS using  
401 this array.

#### 402 **4.7 Stanford 3 - Stanford Campus with two IUs**

403 Stanford 3 was a temporary dual IU experiment on Stanford campus between October  
404 5, 2017 and October 13, 2017, using the same Stanford 1 cable loop. Besides the OptaSense  
405 ODH-3 model that recorded since 2016, this experiment attached an additional IU, the

406 OptaSense ODH-4 model, that started interrogating using acquisition parameters iden-  
 407 tical to the ODH-3. Both IUs collected data concurrently using the same settings for three  
 408 days, and then a set of various gauge lengths and sampling rates were tested on the ODH-  
 409 4 individually. The experiment shows better data quality in ODH-4 recordings than ODH-  
 410 3, and the high-quality ODH-4 data were used for H/V spectral ratio analysis (Z. J. Spica,  
 411 Pertont, et al., 2020). Three broadband seismometers were contemporaneously installed  
 412 in building basements by the USGS within the cable loop (U.S. Geological Survey, 2016)  
 413 and collected ground motion data for comparison.

#### 414 4.8 Valencia Array

415 The Valencia-Islalink experiment (Z. Spica et al., 2020) used a pre-installed telecommu-  
 416 nication fiber-optic cable operated by IslaLink Holding Iberia S.L. and connecting the  
 417 Spanish peninsula to Mallorca Island from Valencia to Palma de Mallorca (Fig. 7). From  
 418 September 1st to September 15th, 2020, a Febus Optics IU was connected to the Valen-  
 419 cia side to sample the first 50 km of the cable. The cable location provided by the ca-  
 420 ble operator, indicates that the first 9,189 m are on land. This is easily confirmed with  
 421 the observation of characteristic traffic noise in the record sections. According to the in-  
 422 stallation report, the remaining 40,811 m are buried  $\sim 1$  m below the Mediterranean seabed.

423 This is also confirmed  
 424 by the observation of  
 425 strong marine grav-  
 426 ity waves and the sec-  
 427 ondary microseism in  
 428 the record sections (Xiao  
 429 et al., 2022). Data were  
 430 acquired at a sampling  
 431 frequency of 1000 Hz,  
 432 with a gauge length  
 433 of 30 m and a spatial  
 434 resolution of 16.8 m,  
 435 resulting in a dense seis-  
 436 mic array of 2977 channels. The data from September 1st to September 7th are contin-

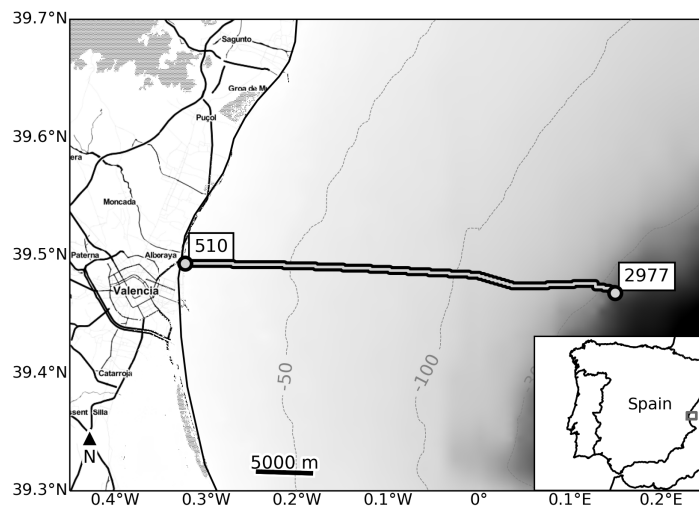


**Figure 7.** Map of the Valencia arrays showing the undersea channels.

437 vious and available on PubDAS. The remaining week was less complete with the pres-  
438 ence of numerous recording gaps and was therefore not published.

## 439 **5 Metadata**

440 To measure Earth vibrations with DAS, fiber-optic cables should be fully coupled to the  
441 ground. In principle, good coupling with the surrounding medium can be obtained by  
442 burying cables in the ground and detailed logs of the burial process should be made avail-  
443 able. In practice, cables might not be locally coupled to the ground (e.g., cables locally  
444 hanging along electricity lines or zip-tied loops in man-holes) and coupling conditions  
445 are generally unknown or poorly constrained. In addition, DAS measurements of a fully  
446 coupled cable are impacted by the cable manufacturing properties. For example, cables  
447 deployed on the ocean floor need to withstand extreme pressure conditions, and are typ-  
448 ically heavier with multiple fiber strands, a steel jacket, and a copper core. This contrasts  
449 with cables laying at the surface of the Earth, which can simply be protected by a thick  
450 plastic jacket, and borehole deployments, which sometimes include specific components  
451 to avoid fiber breakage during deployment. The design of optical fibers also controls the  
452 sensitivity of the measurement and other features, such as polarization and attenuation.  
453 In addition to fiber/cable manufacturing properties, information about potential splic-  
454 ing of the fiber is critical as it can dramatically increase the attenuation along the fiber.  
455 Finally, locating the precise position of the DAS channels is essential for Earth science  
456 purposes. GPS and tap tests (or airguns in oceans; Takano et al. (2021)) are used to pre-  
457 cisely locate channels; however, when working with telecommunication cables, details about  
458 the cable deployments are often uncertain and incomplete, or even classified.

459 Most IUs are patented, and the exact details on their working principles, optical chains,  
460 and running algorithms are not fully accessible to users. While all IUs use laser pulses,  
461 the physical properties of such pulses may differ (repetition rate, length, and shape of  
462 the pulses), leading to a different signal (e.g., strain, strain-rate, phases) over a broad  
463 range of measurement lengths. Moreover, some IUs pre-process raw data on the fly be-  
464 fore writing them to a hard drive while other IUs simply save the raw data. Depending  
465 on the system, some parameters may be adjustable or fixed and imposed (e.g., the gauge  
466 length) by the manufacturing design of the IU. Finally, IUs can easily be switched and  
467 several IUs can be used on one single cable.

468 During an ideal measurement campaign, analysts should collect both the fiber and as-  
469 sociated cable metadata as well as the IU metadata, including acquisition parameters.  
470 Due to the large range of parameters described above, a single measurement campaign  
471 can result in the collection of a large volume of metadata. Therefore, standard seismic  
472 metadata (e.g., SEED) and file formats (e.g., SAC, SEG-Y) are not well-suited for DAS  
473 experiments because they cannot hold all the acquisition parameters needed for the proper  
474 characterization of an experiment. Obtaining a metadata model that fits all the require-  
475 ments for DAS experiments is challenging and still open to discussion. Recently, Mellors  
476 et al. (2022) and the Data Management Working Group from the DAS Research Coordi-  
477 nation Network suggested a first version of a common metadata standard for archival  
478 purposes, regardless of the data format. In an effort to test, improve, and standardize  
479 the DAS metadata, the PubDAS team follows these guidelines and each dataset comes  
480 with a pdf document called 'Metadata'. The 'Metadata' files are purely parameter-oriented  
481 and allow the end user to have a quick overview of the measurement parameters, when  
482 available or known. Note that the metadata files contain fields that are left blank when  
483 the information is unknown for a given dataset. For additional details about metadata  
484 files, structure, and description of the parameters, we refer the reader to Mellors et al.  
485 (2022). While a standardized metadata architecture offers some structure and coherence  
486 among datasets, it does not provide useful recommendations for the end user to start  
487 processing the data. Therefore, each dataset comes with a complementary 'README'  
488 file that provides more practical information about the data, such as which script to use  
489 to read the files, a list of citable references, a link to a license file, acknowledgments, or  
490 detailed explanation about the various files (other than DAS) shared in a directory.

## 491 **6 How to access PubDAS**

492 PubDAS is hosted by the Advanced Research Computing division of the Information and  
493 Technology Services at the University of Michigan (UM). The repository is located on  
494 a cost-optimized, high-capacity, and large-file storage service called *Locker*. PubDAS is  
495 accessible through *Globus*, which is a non-profit software as-a-service provider (Foster,  
496 2011), using the link provided in the Data and Resources section. Globus is free, easy-  
497 to-use, and provides secure and high-performance file transfer between storage systems  
498 (Chard et al., 2017; Ananthakrishnan et al., 2015). In short, Globus can be seen as self-  
499 service data portal and point-and-click data management tool that allows researchers

500 to focus more on science and less on technology. It is rapidly being adopted by many large  
501 institutions across the globe such as Amazon Web Services, the National Science Foun-  
502 dation XSEDE systems, and many US national laboratories and universities.

503 Globus facilitates data transfer by handling all the complex aspects of large-scale trans-  
504 fer. For example, it uses multiple parallel Transmission Control Protocol (TCP) streams  
505 to achieve high throughput, and automatically tunes parameters to maximize bandwidth  
506 usage without interfering with current use. Globus also coordinates authentication at  
507 source and destination while providing automatic fault recovery, and notifies users of com-  
508 pletions and problems. While Globus cloud-hosted service coordinates data transfers,  
509 the end-user only relies on the *Globus Connect Personal* software to enable fast and re-  
510 liable data transfers between institutional servers or personal workstations. The Globus  
511 Connect Personal software is available as a lightweight single-user agent that can be eas-  
512 ily deployed on Windows, Mac, and Linux computers. Globus Connect Server also ex-  
513 ists as a multi-user server available as a native linux package. Users are also able to use  
514 Globus python API clients for data access and transfer. After downloading and installing  
515 the software, users must register their desired storage as a Globus “endpoint”, which uniquely  
516 identifies and maps the data access interface. The endpoint also includes metadata such  
517 as ownership, name, and other descriptions. Once the endpoint is set up either on a server  
518 or a personal workstation, end-users can download the PubDAS data set of their choice.  
519 A link toward a step-by-step guide on “how to log into Globus and use it to transfer files”  
520 is provided in the Data and Resources section.

521 Globus Connect Personal is designed to work automatically with common firewall set-  
522 tings. However, very strict firewall policies – i.e., the ones that block outbound connec-  
523 tions – will hinder this behavior. In this case, the end users may have to work with their  
524 network or security administrators to open specific outbound TCP and User Datagram  
525 Protocol (UDP) ports. A link explaining how to configure the firewall policy for Globus  
526 Connect Personal is also provided in the Data and Resources section.

527 Currently, the UM has 400 Gbps of internet bandwidth allowing up to several PB/day  
528 of file transfer between multiple devices and multiple locations simultaneously. Of course,  
529 the download of data will critically depend on available end-user bandwidth. For this  
530 reason, when possible, we recommend use of an institutional fiber connection rather than  
531 home internet for dataset retrieval. We have tested download and upload speeds for sev-  
532 eral data sets between institutions. A summary of our experience is shown in Table 2.

533 These results shows that even with a low-speed connection (e.g.,  $\sim 20$ mb/s), the opti-  
 534 mization of the data transfer with Globus still provides performance acceptable for re-  
 535 trieving the test datasets.

Origin	Destination	Files transferred	Bytes transferred	Effective Speed (MB/s)	Time
UM	CSM	1585	509.02 GB	491.76	17 m 15 s
UM	UNAM	2744	5.94 TB	102.73	16 h 5 m 5 s
IGN	UM	1	240.08 GB	29.05	2 h 15 m 55 s
ERI	UM	7389	15.64 TB	90.81	1 d 23 h 50 m 40 s
CTC	UM	8868	2.91 TB	21.74	1 d 13 h 17 m 27 s
UM	Caltech	3241	1.08 TB	163.22	1 h 51 m 8 s

**Table 2.** Examples of data upload and download using Globus and using different network speeds. UM: University of Michigan; CSM: Colorado School of Mines, USA; UNAM: Universidad Nacional Autónoma de México, Mexico; IGN: Instituto Geográfico Nacional, Spain; ERI: Earthquake Research Institute, Japan; CTC: Cordova Telephone Cooperative, Alaska, USA; Caltech: California Institute of Technology, USA.

## 536 7 Public DAS Data Beyond PubDAS

537 Many researchers and institutions have started to share their DAS datasets with the sci-  
 538 entific community. For example, the Department of Energy’s GDR, hosts two frequently  
 539 cited DAS datasets – PoroTomo (University of Wisconsin, 2016) and FORGE 2C (University  
 540 of Utah Seismograph Stations, 2022). Yet, while tens of terabytes of data have already  
 541 been made available online, research groups generally publish individual datasets. The  
 542 lack of a centralized platform makes it difficult for the end user to navigate the flow of  
 543 information and the complexity of each platform since every dataset has its own require-  
 544 ments, its own metadata reporting, and might not be equally advertised to the broader  
 545 scientific community. In an effort to centralize the available datasets online and acknowl-  
 546 edge the work of our peers, we summarize their availability in Table 3. Note that only  
 547 relatively large datasets are reported. Small data examples shared to support the works  
 548 published in journal publications are not reported. For more information about these  
 549 datasets, we invite the reader to refer to the url’s provided in Table 3.

Short Name	Approx. Vol. (Gb)	Location	T. Span (d)	Access
DAS4Microseism	182	Svalbard, Norway	42	doi:10.18710/VPRD2H
DAS4Whale	37.6	Svalbard, Norway	2	doi:10.5281/zenodo.5823343
RAPID	26,000	Offshore Pacific City, OR	5	piweb.ooirsn.uw.edu/das/
Porotomo*	81,000	Brady Hot Springs, NV	15	doi:10.15121/1778858
FORGE 2C*	~	Milford, Utah	~	tinyurl.com/2p8epnn5
Marcellus*	~	Morgantown, WV	~	www.mseel.org/
Garner Valley*	165	California	1	doi:10.15121/1261941
Levee Workshop*	0.741	Black Hawk, LA	1	doi:10.17603/ds2-c96x-pg70
Belgium	1.3	Zeebrugge, Belgium	1	doi:10.22002/D1.1296
Monterey Bay	0.565	Moss Landing, CA	4	tinyurl.com/ynab86bc
SAFOD	1.54	San Andreas Fault, CA	~	tinyurl.com/yc49swp4
FORESEE	28,670	State College, PA	180	tinyurl.com/499mn4pa

**Table 3.** Non-exhaustive list of other DAS datasets available for download on other platforms. A  $\star$  means that the data contain active sources. A  $\sim$  means that this value may vary or is unknown.

## 550 8 Conclusions and future steps

551 This paper presents the first large-scale open-source repository where several DAS datasets  
552 from multiple application areas are publically shared. The individual datasets have been  
553 curated and organized to provide more structure to scientists keen to explore new fron-  
554 tiers in geosciences. All the datasets have already been tested and explored to some ex-  
555 tent, which resulted in several publications ensuring that the quality of the recorded sig-  
556 nals is sufficient for many seismological applications. Nonetheless, some datasets have  
557 only been explored superficially, offering tremendous opportunities for new discoveries  
558 by other research groups without current DAS data access. For example, we believe that  
559 some of the datasets can be used to understand the relationship between DAS and con-  
560 ventional seismometry, to provide further constraints on fault zones and dynamic envi-  
561 ronmental changes, and to develop new tools for urban monitoring. In addition, we hope  
562 that the open-access component of this project will accelerate progress in seismology and  
563 geosciences and facilitate training, validation, and performance comparisons. More im-  
564 portantly, we hope that PubDAS will ease the adoption of best practices when using DAS

565 data, and allow a broader community to take part in the ongoing efforts to better un-  
566 derstand the Earth.

567 Currently,  $\sim 90$  TB of DAS data are hosted at the University of Michigan, and there are  
568 plans to add new datasets upon the conclusion of some experiments and publication em-  
569 bargoes. The PubDAS team has secured support through the end of 2026 and will con-  
570 tinue exploring possibilities to share these data in the long term. In parallel, we will seek  
571 opportunities to collaborate with more recognized data centers that could host the rapidly  
572 increasing amount of DAS data recorded around the world.

573 With terabytes of data being collected daily around the world, seismology is more than  
574 ever a data-driven science. DAS and optical fiber sensing in general open a new chap-  
575 ter in resolving fine scale variations of the seismic wavefield that were until recently un-  
576 observable, making the technology one of the greatest advances in geophysical instru-  
577 mentation since digitization. Along with recent breakthroughs in high-performance com-  
578 puting and machine/deep learning, DAS is now offering the big data essential to expand  
579 our knowledge of the physics behind Earth's heterogeneous interior and surface processes.  
580 We hope that PubDAS will act as a bridge between scientific communities and will fa-  
581 cilitate the accessibility to a broader and more diverse body of knowledge.

## 582 **9 Data and Resources**

583 The PubDAS Globus endpoint at UM is accessible via the following link: [https://app](https://app.globus.org/file-manager?origin_id=706e304c-5def-11ec-9b5c-f9dfb1abb183&origin_path=%2F)  
584 [.globus.org/file-manager?origin\\_id=706e304c-5def-11ec-9b5c-f9dfb1abb183&origin](https://app.globus.org/file-manager?origin_id=706e304c-5def-11ec-9b5c-f9dfb1abb183&origin_path=%2F)  
585 [\\_path=%2F](https://app.globus.org/file-manager?origin_id=706e304c-5def-11ec-9b5c-f9dfb1abb183&origin_path=%2F). Instructions to download and run Globus Connect Personal are accessible  
586 via the following link: [www.globus.org/globus-connect-personal](http://www.globus.org/globus-connect-personal) Globus Connect Per-  
587 sonal basic tutorial is also available on Youtube via the following link [www.youtube.com/](http://www.youtube.com/watch?v=bpnVcAN99WY)  
588 [watch?v=bpnVcAN99WY](http://www.youtube.com/watch?v=bpnVcAN99WY) The step-by-step guide to log in and transfer files with Globus  
589 is accessible via the following link: [docs.globus.org/how-to/get-started/](https://docs.globus.org/how-to/get-started/). The fire-  
590 wall policy for Globus Connect Personal is accessible via the following link: [docs.globus](https://docs.globus.org/how-to/configure-firewall-gcp/)  
591 [.org/how-to/configure-firewall-gcp/](https://docs.globus.org/how-to/configure-firewall-gcp/). The complete Globus documentation is ac-  
592 cessible via the following link [docs.globus.org/](https://docs.globus.org/). For any question about Globus, please  
593 work directly with your Information and Technology specialists.

## 594 **Acknowledgments**

595 The PubDAS project was initiated by the Air Force Research Laboratory through grant  
 596 FA9453-21-2-0018. We are thankful to all the persons involved in the DAS data collec-  
 597 tions around the world. This includes our industry partners who either provided the IUs  
 598 or access to telecommunication cables. It also includes all the researchers, students, en-  
 599 gineers, field technicians and information and technology specialists who gave some of  
 600 their time to these experiments and without whom PubDAS wouldn't have been posi-  
 601 sible. We particularly want to thank Brock Palen and Michael Messina from the Advanced  
 602 Research Computing at University of Michigan, who helped to build and host the Pub-  
 603 DAS repository. We would like to thank Abdul Hafiz Issah for testing Globus PubDAS  
 604 download speeds. We thank Robert Mellors, Kathleen Hodgkinson, and Voon Hui Lai  
 605 for interesting discussions about the metadata. We also thank the anonymous authors  
 606 of the Google Document "Publicly Available DAS Data Overview", that helped to write  
 607 section 7. L.V was supported by NSF award EAR2022716. The manuscript has a Los  
 608 Alamos National Laboratory Unlimited Release Number (LA-UR-22-29228).

609 **Competing interests:** The authors declare that they have no competing interests.

## 610 **References**

- 611 Ajo-Franklin, J., Dou, S., Daley, T., Freifeld, B., Robertson, M., Ulrich, C., . . . oth-  
 612 ers (2017). Time-lapse surface wave monitoring of permafrost thaw using  
 613 distributed acoustic sensing and a permanent automated seismic source. In  
 614 *Seg technical program expanded abstracts 2017* (pp. 5223–5227). Society of  
 615 Exploration Geophysicists.
- 616 Ajo-Franklin, J. B., Dou, S., Lindsey, N. J., Monga, I., Tracy, C., Robertson, M., . . .  
 617 Li, X. (2019). Distributed acoustic sensing using dark fiber for near-surface  
 618 characterization and broadband seismic event detection. *Scientific reports*,  
 619 *9*(1), 1328.
- 620 Ananthkrishnan, R., Chard, K., Foster, I., & Tuecke, S. (2015). Globus platform-  
 621 as-a-service for collaborative science applications. *Concurrency and Computa-*  
 622 *tion: Practice and Experience*, *27*(2), 290–305.
- 623 Bakku, S. K. (2015). *Fracture characterization from seismic measurements in a bore-*  
 624 *hole* (Unpublished doctoral dissertation). Massachusetts Institute of Technol-  
 625 ogy.

- 626 Ben-Zion, Y., Vernon, F. L., Ozakin, Y., Zigone, D., Ross, Z. E., Meng, H., . . .  
 627 Barklage, M. (2015). Basic data features and results from a spatially dense  
 628 seismic array on the San Jacinto fault zone. *Geophysical Journal International*,  
 629 *202*(1), 370–380.
- 630 Biondi, B., Clapp, R. G., Yuan, S., & Huot, F. (2021). Scaling up to city-wide  
 631 dark-fiber seismic arrays: Lessons from five years of the stanford das array  
 632 project. In *First international meeting for applied geoscience & energy* (pp.  
 633 3225–3229).
- 634 Biondi, B., Martin, E., Cole, S., Karrenbach, M., & Lindsey, N. (2017). Earth-  
 635 quakes analysis using data recorded by the Stanford DAS Array. In *Seg tech-*  
 636 *nical program expanded abstracts 2017* (pp. 2752–2756). Society of Exploration  
 637 Geophysicists.
- 638 Boué, P., Poli, P., Campillo, M., Pedersen, H., Briand, X., & Roux, P. (2013). Tele-  
 639 seismic correlations of ambient seismic noise for deep global imaging of the  
 640 earth. *Geophysical Journal International*, ggt160.
- 641 Castellanos, J. C., Clayton, R. W., & Juarez, A. (2020). Using a time-based  
 642 subarray method to extract and invert noise-derived body waves at Long  
 643 Beach, California. *Journal of Geophysical Research: Solid Earth*, *125*(5),  
 644 e2019JB018855.
- 645 Chard, K., Foster, I., & Tuecke, S. (2017). Globus: Research data management as  
 646 service and platform. In *Proceedings of the practice and experience in advanced*  
 647 *research computing 2017 on sustainability, success and impact* (pp. 1–5).
- 648 Cheng, F., Chi, B., Lindsey, N. J., Dawe, T. C., & Ajo-Franklin, J. B. (2021). Uti-  
 649 lizing distributed acoustic sensing and ocean bottom fiber optic cables for  
 650 submarine structural characterization. *Scientific reports*, *11*(1), 1–14.
- 651 Cheng, F., Lindsey, N. J., Sobolevskaia, V., Dou, S., Freifeld, B., Wood, T., . . . Ajo-  
 652 Franklin, J. B. (n.d.). Watching the cryosphere thaw: Seismic monitoring of  
 653 permafrost degradation using distributed acoustic sensing during a controlled  
 654 heating experiment. *Geophysical Research Letters*, e2021GL097195.
- 655 Currenti, G., Jousset, P., Napoli, R., Krawczyk, C., & Weber, M. (2021). On the  
 656 comparison of strain measurements from fibre optics with a dense seismometer  
 657 array at Etna volcano (Italy). *Solid Earth*, *12*(4), 993–1003.
- 658 Daley, T. M., Freifeld, B. M., Ajo-Franklin, J., Dou, S., Pevzner, R., Shulakova, V.,

- 659 ... Lueth, S. (2013). Field testing of fiber-optic distributed acoustic sensing  
660 (DAS) for subsurface seismic monitoring. *The Leading Edge*, 32(6), 699–706.
- 661 Dean, T., Cuny, T., & Hartog, A. H. (2017). The effect of gauge length on axially  
662 incident P-waves measured using fibre optic distributed vibration sensing. *Geo-  
663 physical Prospecting*, 65(1), 184–193.
- 664 Dou, S., Lindsey, N., Wagner, A. M., Daley, T. M., Freifeld, B., Robertson, M., ...  
665 Ajo-Franklin, J. B. (2017). Distributed acoustic sensing for seismic monitoring  
666 of the near surface: A traffic-noise interferometry case study. *Scientific reports*,  
667 7(1), 11620.
- 668 Fang, G., Li, Y. E., Zhao, Y., & Martin, E. R. (2020). Urban near-surface seis-  
669 mic monitoring using distributed acoustic sensing. *Geophysical Research Let-  
670 ters*, 47(6), e2019GL086115.
- 671 Fichtner, A., Klaasen, S., Thrastarson, S., Çubuk-Sabuncu, Y., Paitz, P., &  
672 Jónsdóttir, K. (2022). Fiber-optic observation of volcanic tremor through  
673 floating ice sheet resonance. *The Seismic Record*, 2(3), 148–155.
- 674 Foster, I. (2011). Globus online: Accelerating and democratizing science through  
675 cloud-based services. *IEEE Internet Computing*, 15(3), 70–73.
- 676 Grattan, K., & Sun, T. (2000). Fiber optic sensor technology: an overview. *Sensors  
677 and Actuators A: Physical*, 82(1-3), 40–61.
- 678 Hammond, J. O., England, R., Rawlinson, N., Curtis, A., Sigloch, K., Harmon, N.,  
679 & Baptie, B. (2019). The future of passive seismic acquisition. *Astronomy &  
680 Geophysics*, 60(2), 2–37.
- 681 Hartog, A. H. (2017). *An introduction to distributed optical fibre sensors*. CRC  
682 press.
- 683 Hone, S., & Zhu, T. (2021). Seismic observations of four thunderstorms using an un-  
684 derground fiber-optic array. *Seismological Research Letters*, 92(4), 2389–2398.
- 685 Hudson, T. S., Baird, A. F., Kendall, J.-M., Kufner, S.-K., Brisbourne, A. M.,  
686 Smith, A. M., ... Clarke, A. (2021). Distributed Acoustic Sensing (DAS)  
687 for natural microseismicity studies: A case study from Antarctica. *Journal of  
688 Geophysical Research: Solid Earth*, 126(7), e2020JB021493.
- 689 Huot, F., & Biondi, B. (2018). Machine learning algorithms for automated seismic  
690 ambient noise processing applied to DAS acquisition. In *2018 seg international  
691 exposition and annual meeting*.

- 692 Huot, F., Ma, Y., Cieplicki, R., Martin, E., & Biondi, B. (2017). Automatic noise  
693 exploration in urban areas. In *Seg technical program expanded abstracts 2017*  
694 (pp. 5027–5032). Society of Exploration Geophysicists.
- 695 IRIS. (2022). *IRIS DMC Data Statistics*. Retrieved September 2022, from [https://](https://ds.iris.edu/data/distribution/)  
696 [ds.iris.edu/data/distribution/](https://ds.iris.edu/data/distribution/)
- 697 Iten, M. (2012). *Novel applications of distributed fiber-optic sensing in geotechnical*  
698 *engineering* (Vol. 19632). vdf Hochschulverlag AG.
- 699 Jousset, P., Currenti, G., Schwarz, B., Chalari, A., Tilmann, F., Reinsch, T., ...  
700 Krawczyk, C. M. (2022). Fibre optic distributed acoustic sensing of volcanic  
701 events. *Nature communications*, *13*(1), 1–16.
- 702 Jousset, P., Reinsch, T., Ryberg, T., Blanck, H., Clarke, A., Aghayev, R., ...  
703 Krawczyk, C. M. (2018). Dynamic strain determination using fibre-optic  
704 cables allows imaging of seismological and structural features. *Nature commu-*  
705 *nications*, *9*(1), 2509.
- 706 Karrenbach, M., Kahn, D., Cole, S., Ridge, A., Boone, K., Rich, J., ... Langton,  
707 D. (2017). Hydraulic-fracturing-induced strain and microseismic using in situ  
708 distributed fiber-optic sensing. *The Leading Edge*, *36*(10), 837–844.
- 709 Klaasen, S., Thrastarson, S., Jonsdottir, K., Sabuncu, Y. C., Paitz, P., & Ficht-  
710 ner, A. (2021). Distributed acoustic sensing on volcanoes: Grímsvötn and  
711 Fagradalsfjall, Iceland. In *Agu fall meeting*.
- 712 Kong, Q., Trugman, D. T., Ross, Z. E., Bianco, M. J., Meade, B. J., & Gerstoft, P.  
713 (2019). Machine learning in seismology: Turning data into insights. *Seismolog-*  
714 *ical Research Letters*, *90*(1), 3–14.
- 715 Lancelle, C. E., Baldwin, J. A., Lord, N., Fratta, D., Chalari, A., & Wang, H. F.  
716 (2021). Using Distributed Acoustic Sensing (DAS) for Multichannel Analy-  
717 sis of Surface Waves (MASW). *Distributed Acoustic Sensing in Geophysics:*  
718 *Methods and Applications*, 213–228.
- 719 Lay, T., Williams, Q., & Garnero, E. J. (1998). The core–mantle boundary layer and  
720 deep Earth dynamics. *Nature*, *392*(6675), 461–468.
- 721 Lellouch, A., Horne, S., Meadows, M. A., Farris, S., Nemeth, T., & Biondi, B.  
722 (2019). DAS observations and modeling of perforation-induced guided waves in  
723 a shale reservoir. *The Leading Edge*, *38*(11), 858–864.
- 724 Lellouch, A., Yuan, S., Spica, Z., Biondi, B., & Ellsworth, W. (2019a). A Moveout-

- 725 Based Method for the Detection of Weak Seismic Events Using Downhole DAS  
726 Arrays. In *81st eage conference and exhibition 2019*.
- 727 Lellouch, A., Yuan, S., Spica, Z., Biondi, B., & Ellsworth, W. (2019b). Seismic  
728 velocity estimation using passive downhole distributed acoustic sensing records  
729 - examples from the San Andreas Fault Observatory at Depth. *Journal of*  
730 *Geophysical Research (Solid Earth)*. doi: 10.1029/2019JB017533
- 731 Li, Y., Karrenbach, M., & Ajo-Franklin, J. B. (2021). A Literature Review: Dis-  
732 tributed Acoustic Sensing (DAS) Geophysical Applications Over the Past 20  
733 Years. *Distributed Acoustic Sensing in Geophysics: Methods and Applications*,  
734 229–291.
- 735 Li, Z., & Zhan, Z. (2018). Pushing the limit of earthquake detection with distributed  
736 acoustic sensing and template matching: a case study at the brady geothermal  
737 field. *Geophysical Journal International*, *215*(3), 1583–1593.
- 738 Lindsey, N. J., Dawe, T. C., & Ajo-Franklin, J. B. (2019). Illuminating seafloor  
739 faults and ocean dynamics with dark fiber distributed acoustic sensing. *Sci-*  
740 *ence*, *366*(6469), 1103–1107.
- 741 Lindsey, N. J., & Martin, E. R. (2021). Fiber-optic seismology. *Annual Review*  
742 *of Earth and Planetary Sciences*, *49*, 309–336. doi: 10.1146/annurev-earth  
743 -072420-065213
- 744 Lindsey, N. J., Martin, E. R., Dreger, D. S., Freifeld, B., Cole, S., James, S. R., ...  
745 Ajo-Franklin, J. B. (2017). Fiber-optic network observations of earthquake  
746 wavefields. *Geophysical Research Letters*, *44*(23), 11–792.
- 747 Lindsey, N. J., Rademacher, H., & Ajo-Franklin, J. B. (2020). On the broadband in-  
748 strument response of fiber-optic DAS arrays. *Journal of Geophysical Research:*  
749 *Solid Earth*, *125*(2), e2019JB018145.
- 750 Lindsey, N. J., Yuan, S., Lellouch, A., Gualtieri, L., Lecocq, T., & Biondi, B. (2020).  
751 City-scale dark fiber DAS measurements of infrastructure use during the  
752 COVID-19 pandemic. *Geophysical research letters*, *47*(16), e2020GL089931.
- 753 Lior, I., Sladen, A., Rivet, D., Ampuero, J.-P., Hello, Y., Becerril, C., ... Chris-  
754 tos, M. (2021). On the Detection Capabilities of Underwater Distributed  
755 Acoustic Sensing. *Journal of Geophysical Research: Solid Earth*, *126*(3),  
756 e2020JB020925. doi: 10.1029/2020JB020925
- 757 Martin, E., Biondi, B., Cole, S., & Karrenbach, M. (2017). *Overview of the Stanford*

- 758 *DAS Array-1 (SDASA-1)*. Stanford Exploration Project.
- 759 Martin, E., Biondi, B., Karrenbach, M., & Cole, S. (2017). Continuous subsurface  
760 monitoring by passive seismic with distributed acoustic sensors-the “Stanford  
761 array” experiment. In *15th international congress of the brazilian geophysical  
762 society & expogef, rio de janeiro, brazil, 31 july-3 august 2017* (pp. 1366–  
763 1370).
- 764 Martin, E. R. (2018). *Passive imaging and characterization of the subsurface with  
765 distributed acoustic sensing* (open access PhD dissertation). Stanford Univer-  
766 sity.
- 767 Martin, E. R., & Biondi, B. L. (2017). Ambient noise interferometry across two-  
768 dimensional DAS arrays. In *Seg technical program expanded abstracts 2017*  
769 (pp. 2642–2646). Society of Exploration Geophysicists.
- 770 Martin, E. R., & Biondi, B. L. (2018). Eighteen months of continuous near-surface  
771 monitoring with DAS data collected under Stanford University. In *Seg techni-  
772 cal program expanded abstracts 2018* (pp. 4958–4962). Society of Exploration  
773 Geophysicists.
- 774 Martin, E. R., Castillo, C. M., Cole, S., Sawasdee, P. S., Yuan, S., Clapp, R., ...  
775 Biondi, B. L. (2017). Seismic monitoring leveraging existing telecom infras-  
776 tructure at the SDASA: Active, passive, and ambient-noise analysis. *The  
777 Leading Edge*, *36*(12), 1025–1031.
- 778 Martin, E. R., Huot, F., Ma, Y., Cieplicki, R., Cole, S., Karrenbach, M., & Biondi,  
779 B. L. (2018). A seismic shift in scalable acquisition demands new processing:  
780 Fiber-optic seismic signal retrieval in urban areas with unsupervised learning  
781 for coherent noise removal. *IEEE Signal Processing Magazine*, *35*(2), 31–40.
- 782 Martin, E. R., Lindsey, N., Ajo-Franklin, J., & Biondi, B. (2018). Introduction to in-  
783 terferometry of fiber optic strain measurements. *EarthArXiv*. doi: 10.31223/  
784 osf.io/s2tjd
- 785 Mateeva, A., Lopez, J., Mestayer, J., Wills, P., Cox, B., Kiyashchenko, D., ...  
786 Grandi, S. (2013). Distributed acoustic sensing for reservoir monitoring  
787 with VSP. *The Leading Edge*, *32*(10), 1278–1283.
- 788 Mateeva, A., Mestayer, J., Cox, B., Kiyashchenko, D., Wills, P., Lopez, J., ... Roy,  
789 J. (2012). Advances in distributed acoustic sensing (DAS) for VSP. In *Seg  
790 technical program expanded abstracts 2012* (pp. 1–5). Society of Exploration

- 791 Geophysicists.
- 792 Mateeva, A., Mestayer, J., Yang, Z., Lopez, J., Wills, P., Roy, J., & Bown, T.  
793 (2013). Dual-well 3D VSP in deepwater made possible by DAS. In *Seg techni-*  
794 *cal program expanded abstracts 2013* (pp. 5062–5066). Society of Exploration  
795 Geophysicists.
- 796 Mellors, R. J., Abbott, R., Steedman, D., Podrasky, D., & Pitarka, A. (2021). Mod-  
797 eling subsurface explosions recorded on a distributed fiber optic sensor. *Jour-*  
798 *nal of Geophysical Research: Solid Earth*, *126*(12), e2021JB022690.
- 799 Mellors, R. J., Hodgkinson, K. M., Hui Lai, V., & the DAS Research Coordina-  
800 tion Network Data Management Working Group. (2022, July). Distributed  
801 Acoustic Sensing (DAS) Metadata Model [Computer software manual].
- 802 Mestayer, J., Cox, B., Wills, P., Kiyashchenko, D., Lopez, J., Costello, M., ...  
803 Lewis, A. (2011). Field trials of distributed acoustic sensing for geophysical  
804 monitoring. In *Seg technical program expanded abstracts 2011* (pp. 4253–4257).  
805 Society of Exploration Geophysicists.
- 806 Molenaar, M. M., Hill, D., Webster, P., Fidan, E., & Birch, B. (2012). First down-  
807 hole application of distributed acoustic sensing for hydraulic-fracturing moni-  
808 toring and diagnostics. *SPE Drilling & Completion*, *27*(01), 32–38.
- 809 Mordret, A., Landès, M., Shapiro, N., Singh, S., Roux, P., & Barkved, O. (2013).  
810 Near-surface study at the Valhall oil field from ambient noise surface wave  
811 tomography. *Geophysical Journal International*, *193*(3), 1627–1643.
- 812 Nayak, A., Ajo-Franklin, J., & Team, I. V. D. F. (2021). Measurement of surface-  
813 wave phase-velocity dispersion on mixed inertial seismometer–distributed  
814 acoustic sensing seismic noise cross-correlations. *Bulletin of the Seismological*  
815 *Society of America*, *111*(6), 3432–3450.
- 816 Nishimura, T., Emoto, K., Nakahara, H., Miura, S., Yamamoto, M., Sugimura, S.,  
817 ... Kimura, T. (2021). Source location of volcanic earthquakes and subsur-  
818 face characterization using fiber-optic cable and distributed acoustic sensing  
819 system. *Scientific reports*, *11*(1), 1–12.
- 820 Papp, B., Donno, D., Martin, J. E., & Hartog, A. H. (2017). A study of the geo-  
821 physical response of distributed fibre optic acoustic sensors through laboratory-  
822 scale experiments. *Geophysical Prospecting*, *65*(5), 1186–1204.
- 823 Parker, T., Shatalin, S., & Farhadiroushan, M. (2014). Distributed acoustic sensing–

- 824 a new tool for seismic applications. *first break*, 32(2), 61–69.
- 825 Ramachandran, R., Bugbee, K., & Murphy, K. (2021). From open data to open sci-  
826 ence. *Earth and Space Science*, 8(5), e2020EA001562.
- 827 Reinsch, T., Henniges, J., Götz, J., Jousset, P., Bruhn, D., & Lüth, S. (2015).  
828 Distributed acoustic sensing technology for seismic exploration in magmatic  
829 geothermal areas. In *Proceedings world geothermal congress*.
- 830 Ritsema, J., Heijst, H. J. v., & Woodhouse, J. H. (1999). Complex shear wave ve-  
831 locity structure imaged beneath Africa and Iceland. *Science*, 286(5446), 1925–  
832 1928.
- 833 Rivet, D., de Cacqueray, B., Sladen, A., Roques, A., & Calbris, G. (2021). Prelim-  
834 inary assessment of ship detection and trajectory evaluation using distributed  
835 acoustic sensing on an optical fiber telecom cable. *The Journal of the Acousti-  
836 cal Society of America*, 149(4), 2615–2627.
- 837 Rodríguez Tribaldos, V., & Ajo-Franklin, J. B. (2021). Aquifer monitoring using  
838 ambient seismic noise recorded with distributed acoustic sensing (DAS) de-  
839 ployed on dark fiber. *Journal of Geophysical Research: Solid Earth*, 126(4),  
840 e2020JB021004.
- 841 Schmandt, B., & Clayton, R. W. (2013). Analysis of teleseismic P waves with a  
842 5200-station array in Long Beach, California: Evidence for an abrupt bound-  
843 ary to Inner Borderland rifting. *Journal of Geophysical Research: Solid Earth*,  
844 118(10), 5320–5338.
- 845 Shen, J., & Zhu, T. (2021a). Characterizing urban seismic noise recorded by dis-  
846 tributed acoustic sensing array. In *First international meeting for applied  
847 geoscience & energy expanded abstracts* (p. 3215-3219). Retrieved from  
848 <https://library.seg.org/doi/abs/10.1190/segam2021-3583704.1> doi:  
849 10.1190/segam2021-3583704.1
- 850 Shen, J., & Zhu, T. (2021b). Seismic noise recorded by telecommunication fiber op-  
851 tics reveals the impact of COVID-19 measures on human activity. *The Seismic  
852 Record*, 1(1), 46–55. Retrieved from <https://doi.org/10.1785/0320210008>  
853 doi: 10.1785/0320210008
- 854 Shragge, J., Yang, J., Issa, N., Roelens, M., Dentith, M., & Schediwy, S. (2021).  
855 Low-frequency ambient distributed acoustic sensing (DAS): case study from  
856 Perth, Australia. *Geophysical Journal International*, 226(1), 564–581.

- 857 Sladen, A., Rivet, D., Ampuero, J.-P., De Barros, L., Hello, Y., Calbris, G., &  
 858 Lamare, P. (2019). Distributed sensing of earthquakes and ocean-solid earth  
 859 interactions on seafloor telecom cables. *Nature Communications*, *10*(1), 1–8.
- 860 Soga, K., & Luo, L. (2018). Distributed fiber optics sensors for civil engineering in-  
 861 frastructure sensing. *Journal of Structural Integrity and Maintenance*, *3*(1), 1-  
 862 21. Retrieved from <https://doi.org/10.1080/24705314.2018.1426138> doi:  
 863 10.1080/24705314.2018.1426138
- 864 Spica, Z., Gaite, B., & Ruiz Barajas, S. (2020). *The Valencia-Islalink Distributed*  
 865 *Acoustic Sensing Experiment*. PubDAS. Retrieved from [https://www.fdsn](https://www.fdsn.org/networks/detail/ZH.2020/)  
 866 [.org/networks/detail/ZH.2020/](https://www.fdsn.org/networks/detail/ZH.2020/) doi: 10.7914/SN/ZH.2020
- 867 Spica, Z., Perton, M., Nakata, N., Liu, X., & Beroza, G. C. (2018). Shallow  $V_s$  imag-  
 868 ing of the Groningen area from joint inversion of multimode surface waves and  
 869 H/V spectral ratios. *Seismological Research Letters*, *89*(5), 1720–1729. doi:  
 870 10.1785/0220180060
- 871 Spica, Z. J., Castellanos, J. C., Viens, L., Nishida, K., Akuhara, T., Shinohara, M.,  
 872 & Yamada, T. (2022). Subsurface imaging with ocean-bottom distributed  
 873 acoustic sensing and water phases reverberations. *Geophysical Research Let-*  
 874 *ters*, e2021GL095287.
- 875 Spica, Z. J., Nishida, K., Akuhara, T., Pétrélis, F., Shinohara, M., & Yamada,  
 876 T. (2020). Marine sediment characterized by ocean-bottom fiber-optic  
 877 seismology. *Geophysical Research Letters*, *47*(16), e2020GL088360. doi:  
 878 10.1029/2020GL088360
- 879 Spica, Z. J., Perton, M., Martin, E. R., Beroza, G. C., & Biondi, B. (2020). Urban  
 880 seismic site characterization by fiber-optic seismology. *Journal of Geophysical*  
 881 *Research: Solid Earth*, *125*(3), e2019JB018656. doi: 10.1029/2019JB018656
- 882 Sweet, J. R., Anderson, K. R., Bilek, S., Brudzinski, M., Chen, X., DeShon, H., ...  
 883 others (2018). A community experiment to record the full seismic wavefield in  
 884 Oklahoma. *Seismological Research Letters*, *89*(5), 1923–1930.
- 885 Takano, H., Shinohara, M., Nakata, R., Kurashimo, E., Ishiyama, T., & Mochizuki,  
 886 K. (2021). Seismic reflection survey using seafloor optical cable and DAS  
 887 measurement off Sanriku. In *Seismological society of japan fall meeting*.
- 888 Ugalde, A., Becerril, C., Villaseñor, A., Ranero, C. R., Fernández-Ruiz, M. R.,  
 889 Martín-Lopez, S., ... Martins, H. F. (2022). Noise Levels and Signals Ob-

- 890 served on Submarine Fibers in the Canary Islands Using DAS. *Seismological*  
 891 *Research Letters*, 93(1), 351–363.
- 892 University of Utah Seismograph Stations. (2022). *Utah forge das seismic data 2022*  
 893 (Data set). University of Utah Seismograph Stations. Retrieved September  
 894 2022, from <https://gdr.openei.org/submissions/1393>
- 895 University of Wisconsin. (2016). *PoroTomo Natural Laboratory Horizontal and Ver-*  
 896 *tical Distributed Acoustic Sensing Data* (Data set). University of Wisconsin .  
 897 doi: 10.15121/1778858
- 898 U.S. Department of Energy. (2022a). *Energy Data eXchange (EDX)*. Retrieved  
 899 September 2022, from <https://edx.net1.doe.gov/>
- 900 U.S. Department of Energy. (2022b). *Geothermal Data Repository*. Retrieved  
 901 September 2022, from <https://gdr.openei.org/>
- 902 U.S. Geological Survey. (2016). *U.S. Geological Survey Networks. International*  
 903 *Federation of Digital Seismograph Networks. Dataset/Seismic Network. doi:*  
 904 *10.7914/sn/gm* (Tech. Rep.).
- 905 van den Ende, M., & Ampuero, J.-P. (2021). Evaluating seismic beamforming capa-  
 906 bilities of distributed acoustic sensing arrays. *Solid Earth*, 12(4), 915–934.
- 907 Viens, L., Pertou, M., Spica, Z. J., Nishida, K., Shinohara, M., & Yamada, T.  
 908 (2022). Understanding surface-wave modal content for high-resolution  
 909 imaging of submarine sediments with distributed acoustic sensing. *Geo-*  
 910 *physical Journal International (under review - preprint available at*  
 911 *<https://doi.org/10.31223/X5MW7M>*). doi: 10.31223/X5MW7M
- 912 Viens, L., & Spica, Z. J. (2022). Monitoring Ocean Surface Waves Offshore the  
 913 Oregon Coast With Distributed Acoustic Sensing. In *Seismological society of*  
 914 *america, 2022 annual meeting*.
- 915 Wagner, A. M., Lindsey, N. J., Dou, S., Gelvin, A., Saari, S., Williams, C., . . . oth-  
 916 ers (2018). Permafrost degradation and subsidence observations during a  
 917 controlled warming experiment. *Scientific reports*, 8(1), 1–9.
- 918 Walter, F., Gräff, D., Lindner, F., Paitz, P., Köpfl, M., Chmiel, M., & Fichtner,  
 919 A. (2020). Distributed acoustic sensing of microseismic sources and wave  
 920 propagation in glaciated terrain. *Nature communications*, 11(1), 1–10.
- 921 Wang, H. F., Zeng, X., Miller, D. E., Fratta, D., Feigl, K. L., Thurber, C. H., &  
 922 Mellors, R. J. (2018). Ground motion response to an ml 4.3 earthquake using

- 923 co-located distributed acoustic sensing and seismometer arrays. *Geophysical*  
 924 *Journal International*, 213(3), 2020–2036.
- 925 Williams, E. F., Fernández-Ruiz, M. R., Magalhaes, R., Vanthillo, R., Zhan, Z.,  
 926 González-Herráez, M., & Martins, H. F. (2019). Distributed sensing of mi-  
 927 croseisms and teleseisms with submarine dark fibers. *Nature communications*,  
 928 10(1), 1–11.
- 929 Williams, E. F., Fernández-Ruiz, M. R., Magalhaes, R., Vanthillo, R., Zhan, Z.,  
 930 González-Herráez, M., & Martins, H. F. (2021). Scholte wave inversion and  
 931 passive source imaging with ocean-bottom DAS. *The Leading Edge*, 40(8),  
 932 576–583.
- 933 Williams, E. F., Zhan, Z., Martins, H. F., Fernandez-Ruiz, M. R., Martin-Lopez,  
 934 S., Gonzalez-Herraez, M., & Callies, J. (2022). Surface gravity wave inter-  
 935 ferometry and ocean current monitoring with ocean-bottom DAS. *Journal of*  
 936 *Geophysical Research: Oceans*, e2021JC018375.
- 937 Xiao, H., Tanimoto, T., Spica, Z., Gaité, B., Ruiz-Barajas, S., Pan, M., & Viens,  
 938 L. (2022). Locating the precise sources of high-frequency microseisms  
 939 using Distributed Acoustic Sensing. *Geophysical Research Letters*. doi:  
 940 10.1029/2022GL099292
- 941 Yu, C., Zhan, Z., Lindsey, N. J., Ajo-Franklin, J. B., & Robertson, M. (2019). The  
 942 potential of DAS in teleseismic studies: Insights from the Goldstone experi-  
 943 ment. *Geophysical Research Letters*, 46(3), 1320–1328.
- 944 Yuan, S., Lellouch, A., Clapp, R. G., & Biondi, B. (2020). Near-surface character-  
 945 ization using a roadside distributed acoustic sensing array. *The Leading Edge*,  
 946 39(9), 646–653.
- 947 Zeng, X., Lancelle, C., Thurber, C., Fratta, D., Wang, H., Lord, N., ... Clarke, A.  
 948 (2017). Properties of noise cross-correlation functions obtained from a dis-  
 949 tributed acoustic sensing array at Garner Valley, California. *Bulletin of the*  
 950 *Seismological Society of America*, 107(2), 603–610.
- 951 Zeng, X., Wang, H. F., Lord, N., Fratta, D., & Coleman, T. (2021). Field trial  
 952 of distributed acoustic sensing in an active room-and-pillar mine. *Distributed*  
 953 *Acoustic Sensing in Geophysics: Methods and Applications*, 65–79.
- 954 Zhan, Z. (2020). Distributed acoustic sensing turns fiber-optic cables into sensitive  
 955 seismic antennas. *Seismological Research Letters*, 91(1), 1–15.

- 956 Zhu, T., Shen, J., & Martin, E. R. (2021). Sensing Earth and environment dynamics  
957 by telecommunication fiber-optic sensors: an urban experiment in Pennsylva-  
958 nia, USA. *Solid Earth*, *12*(1), 219–235.
- 959 Zhu, T., & Stensrud, D. J. (2019). Characterizing thunder-induced ground motions  
960 using fiber-optic distributed acoustic sensing array. *Journal of Geophysical Re-*  
961 *search: Atmospheres*, *124*(23), 12810–12823.